Available online at www.sciencedirect.com
SCIENCE DIRECT®
Journal of Molecular Catalysis A: Chemical 217 (2004) 103–108
JOURNAL OF MOLECULAR CATALYSIS A: CHEMICAL
www.elsevier.com/locate/molcata

Dehydrogenation of ethylbenzene in the presence of CO_2 over catalysts prepared from hydrotalcite-like precursors

Xingnan Ye [a], Ning Ma [c], Weiming Hua [a], Yinghong Yue [a], Changxi Miao [b], Zaiku Xie [b], Zi Gao [a,*]

[a] *Department of Chemistry and Shanghai Key Laboratory of Molecular Catalysis and Innovative Materials, Fudan University, 220 Handan Road, Shanghai 200433, PR China*
[b] *Shanghai Research Institute of Petrochemical Technology, Shanghai 201208, PR China*
[c] *Department of Chemistry, Shanghai Second Medical University, Shanghai 200025, PR China*

Received 19 December 2003; received in revised form 28 February 2004; accepted 29 February 2004

Available online 26 April 2004

Abstract

Dehydrogenation of ethylbenzene to styrene in the presence of CO_2 was investigated over a series of catalysts prepared by calcination of hydrotalcite-like compounds. Mg/Fe mixed oxide catalysts prepared in this way have high specific surface areas and are active for the dehydrogenation reaction. Incorporation of Al^{3+}, Ni^{2+}, Co^{2+}, and Zn^{2+} into the hydrotalcite-like precursors may further enhance the catalytic activity of the calcined catalysts. The Mg/Zn/Al/Fe catalyst affords the highest ethylbenzene conversion of 53.8% and a styrene selectivity of 96.7% at 773 K. The high catalytic activity and stability of the Mg/Zn/Al/Fe catalyst are attributed to the presence of a larger amount of stronger acid sites and a moderate amount of base sites on the catalyst. The temperature-programmed reduction studies show that the reduction of iron oxide species in the catalysts is retarded after incorporation of Zn^{2+} and Al^{3+}. The higher content of iron oxide species in the catalyst system under reaction conditions favors the redox cycle in the reaction and also enhances the dehydrogenation activity.

Keywords: Hydrotalcite-like compounds; Ethylbenzene dehydrogenation; Styrene; CO_2

1. Introduction

Dehydrogenation of ethylbenzene (EB) over a promoted iron oxide catalyst in the presence of a large excess amount of superheated steam is the current industrial process for producing styrene. Since its main drawbacks are high energy costing and severe cracking, the seeking of an alternative technology is underway worldwide. Oxidative dehydrogenation of EB can be operated at low temperature and it is free from thermodynamic limitations regarding conversion. CO_2 is a mild oxidant as well as a green house gas, and its utilization in the dehydrogenation of alkanes and aromatics has aroused increasing interest. Dehydrogenation of EB in the presence of CO_2 has been studied over a variety of metal oxide catalysts such as iron oxide [1–5], vanadium oxide [6–9], zircomium oxide [10,11], and chromium and cerium oxides [12]. Among these catalysts, the V/MgO catalyst gives the best performance in dehydrogenation of EB [8]. The styrene yield in the presence of CO_2 is 2.5 times higher than that in the absence of CO_2 at 823 K. However, the catalyst deactivates rather quickly. The iron oxide-based and other catalysts are less active for the reaction. In particular, the initial yield of EB in the presence of CO_2 is often lower than that in the presence of inert gases over these catalysts [1,4]. Thus, to develop catalysts with improved dehydrogenation activity and stability is required.

Hydrotalcite-like compounds (HTlcs) have the general formula $[M(II)_{1-x}M(III)_x(OH)_2](A^{n-}_{x/n})\cdot mH_2O$, where M is a metal and A is an anion, usually carbonate in natural minerals. For hydrotalcite-like materials, the metallic cations are homogeneously distributed in the brucite-like layers. Compared to the catalysts prepared by coprecipitation, the catalysts obtained by thermal decomposition of hydrotalcite-like precursors exhibit high surface area, high thermal stability

* Corresponding author. Tel.: +86-2165642792; fax: +86-2165641740.
E-mail address: zigao@fudan.edu.cn (Z. Gao).

1381-1169/$ – see front matter © 2004 Elsevier B.V. All rights reserved.
doi:10.1016/j.molcata.2004.02.024

and highly homogenous metal dispersion [13]. Recently, Mimura et al. [14] reported that calcined hydrotalcite-like compounds display better activity for dehydrogenation of EB in the presence of CO_2 than Fe_2O_3/Al_2O_3 catalyst prepared by coprecipitation method.

In the present work, a series of binary, ternary and quaternary Fe-containing HTlcs were prepared. The catalytic behaviors of the catalysts obtained from calcination of these compounds for dehydrogenation of EB in the presence of CO_2 were investigated and correlated with the results of surface acidity and basicity measurements and temperature-programmed reduction (TPR) tests.

2. Experimental

2.1. Catalyst preparation

The hydrotalcite-like precursors were synthesized using a coprecipitation method similar to that described by Mimura et al. [14]. Solution A was prepared by dissolving the mixture of $M(II)(NO_3)_2$ and $M(III)(NO_3)_3$ in the desired molar ratios in 200 ml of water. Solution B was prepared by dissolving a calculated amount of Na_2CO_3 (according to the relation of $[CO_3^{2-}] = 0.5[M(III)]$) in 100 ml of water. Under vigorous stirring, the solutions of A and B were simultaneously and slowly added into a 500 ml flask, while a 2 M NaOH solution was now and then added to keep the pH in the range of 9.0 ± 0.5. After all the solutions were added, the slurry was stirred for 3 h at 333 K, and then aged for another 24 h. The precipitate was filtered, washed and dried at 393 K overnight. The hydrotalcite-like precursors were calcined at 823 K for 12 in air, unless otherwise noted.

2.2. Characterization

The BET surface areas of the catalysts were measured by N_2 desorption at 77 K on a Micromeritics ASAP 2000 instrument. X-ray powder diffraction (XRD) patterns were recorded on a Rigaku D/MAX-IIA diffractometer with Ni filtered Cu Kα radiation ($\lambda = 1.5406$ Å) operated at 30 kV and 20 mA. TPR experiments were carried out using a Micromeritics TPD/TPR 2900 instrument. Thirty milligrams of catalyst was pretreated in N_2 at 573 K for 3 h. A reduction run was then performed at a heating rate of 10 K min^{-1} under a gas flow (40 ml min^{-1}) of hydrogen (10 vol.%) and argon (90 vol.%). Temperature-programmed desorption of NH_3 (NH_3-TPD) and CO_2 (CO_2-TPD) was performed in a flow-type fix-bed reactor equipped with a thermal conductivity detector (TCD) at atmospheric pressure. Forty milligrams of sample was pretreated at 773 K for 2 h and then cooled to 393 K in He flow for NH_3-TPD or 353 K in He flow for CO_2-TPD. Pure NH_3 or CO_2 was injected until adsorption saturation followed by purging with He for 2 h. The temperature was then raised up from 393 or 353 to 773 K at a rate of 10 K min^{-1} to desorb NH_3 or CO_2.

2.3. Activity test

The dehydrogenation of EB in the presence of CO_2 was carried out in a flow-type fixed-bed microreactor loaded with 200 mg of catalyst under atmospheric pressure. To supply the reactant, a gas mixture of N_2 and CO_2 (19:1 molar ratio) at a flow rate of 60 ml min^{-1} was passed through a glass evaporator filled with liquid EB maintained at 273 K. Prior to the reaction, the catalyst was pretreated at 773 K in N_2 for 2 h unless otherwise stated. The hydrocarbon products were analyzed with a gas chromatograph equipped with a flame ionization detector and a 2 m long stainless steel column packed with 15% DNP. The effluent from the reactor was also collected in a gas bag and analyzed the content of CO and CO_2 with a gas chromatograph equipped with a thermal conductivity detector and a 6 m long stainless steel column packed with porapak Q.

3. Results and discussion

3.1. XRD results

The synthesis of binary Mg/Fe HTlcs was carried out at Mg:Fe molar ratio from 2:1 to 4:1 by coprecipitation method. Substituting Fe^{3+} by Al^{3+}, Mg/Al/Fe HTlcs with various compositions are obtained by the same preparation method. The XRD patterns of the samples are shown in Fig. 1. The peaks at 11.5, 23.1, 34.5, 38.6, 46.5, 59.9, 61.7° are characteristic of the hydrotalcite-like structure.

M(II) ions having ionic radii not too different from that of Mg^{2+} can also form HTlcs [13]. Hydrotalcite-like precursors (Mg/M/Al/Fe = 3/3/1/2) containing Zn^{2+}, Cu^{2+}, Ni^{2+}, Co^{2+}, and Mn^{2+} were prepared. Their XRD patterns are similar to those of Mg/Fe HTlcs.

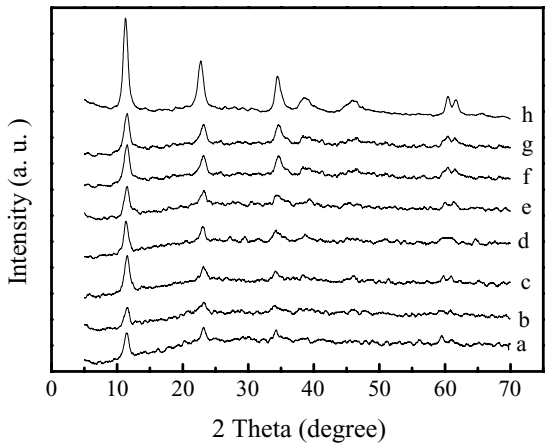

Fig. 1. XRD patterns of Mg/Fe hydrotalcite-like compounds before calcination. (a) Mg/Fe (2/1); (b) Mg/Fe (3/1); (c) Mg/Fe (4/1); (d) Mg/Al/Fe (6/0.5/2.5); (e) Mg/Al/Fe (6/1/2); (f) Mg/Al/Fe (6/1.5/1.5); (g) Mg/Al/Fe (6/2/1); (h) Mg/Al (2/1).

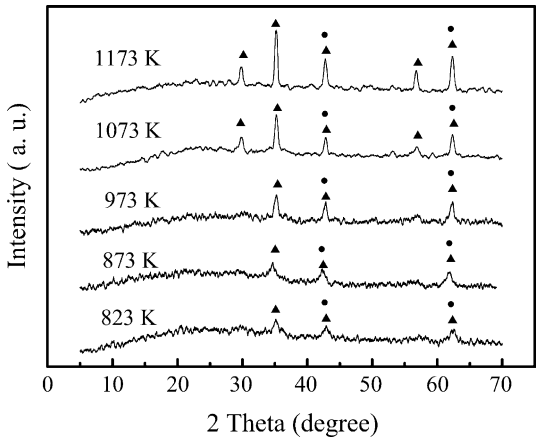

Fig. 2. XRD patterns of the catalyst Mg/Fe (2/1) calcined at different temperatures. (●) MgO; (▲) $MgFe_2O_4$ spinel.

The Mg/Fe (2/1) hydrotalcite-like precursor was calcined at different temperatures. From the XRD patterns of the calcined samples in Fig. 2, three weak broad peaks are observed at 35.4, 42.8, 62.2° for samples calcined below 973 K corresponding to characteristic diffractions of $MgFe_2O_4$ and MgO. As the calcination temperature further increases, the intensities of these peaks are increased and other peaks of $MgFe_2O_4$ at 30 and 57° appear, indicating that the formation of $MgFe_2O_4$ spinel structure is enhanced at high temperature.

The XRD patterns of the ternary and quaternary hydrotalcite-like precursors calcined at 823 K are illustrated in Fig. 3. The diffraction peaks of the calcined Mg/Al/Fe sample are weaker and broader than those of the calcined Mg/Fe sample, indicating that smaller crystallites are formed. This observation is consistent with the results of surface area measurements as shown in Tables 1 and 2. No distinct peak is observed for all the other calcined samples,

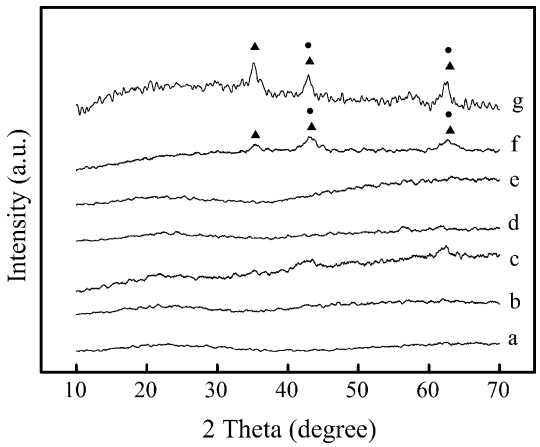

Fig. 3. XRD patterns of ternary and quaternary hydrotalcite-like compounds calcined at 823 K. (a) Mg/Cu/Al/Fe (3/3/1/2); (b) Mg/Mn/Al/Fe (3/3/1/2); (c) Mg/Zn/Al/Fe (3/3/1/2); (d) Mg/Ni/Al/Fe (3/3/1/2); (e) Mg/Co/Al/Fe (3/3/1/2); (f) Mg/Al/Fe (6/1/2); (g) Mg/Fe (2/1). (▲) $MgFe_2O_4$; (●) MgO.

Table 1
Dehydrogenation activity of Mg/Fe catalysts

Catalyst (molar ratio)	Calc. temp. (K)	S_{BET} ($m^2\,g^{-1}$)	EB conv. (%)	Selectivity (%)		
				STY	B	T
Mg/Fe (4/1)	823	83.1	33.2	98.4	1.0	0.6
Mg/Fe (3/1)	823	79.6	34.5	98.6	0.8	0.6
Mg/Fe (2/1)	823	72.5	35.6	99.5	0.5	0
Mg/Fe (2/1)	873	60.8	36.8	99.6	0.4	0
Mg/Fe (2/1)	973	34.2	31.3	99.7	0.3	0
Mg/Fe (2/1)	1073	12.6	15.0	100	0	0
Mg/Fe (2/1)	1173	3.9	5.4	100	0	0

Reaction conditions: 200 mg catalyst; N_2:CO_2:EB = 361:19:1; 773 K; 2 h on stream. EB, ethylbenzene; STY, styrene; B, benzene; T, toluene.

showing that amorphous oxides are formed. It seems that the substitution of Mg^{2+} by other divalent metal cations inhibits the formation of spinel structures during calcination.

3.2. Catalytic performance

The dehydrogenation of EB was carried out in the presence of CO_2 at 773 K over catalysts prepared by calcination of the HTlcs. Styrene is the major product of the reaction, whereas benzene and toluene are minor by-products. The reaction data after 2 h on stream are compared.

The catalytic activities of Mg/Fe catalysts calcined at different temperatures along with the results of surface area measurements are summarized in Table 1. Among the Mg/Fe catalysts with different compositions calcined at 823 K, Mg/Fe (2/1) catalyst gives the highest activity regardless of its low surface area, showing the important role of Fe for the reaction. The activity of the catalysts decreases as the calcination temperature is raised above 873 K. The formation of $MgFe_2O_4$ spinel structure with low surface area at high temperature is probably the cause for the reduction in activity.

The effect of the incorporation of Al^{3+} and various bivalent metal cations into the catalysts on their catalytic

Table 2
Dehydrogenation activity of various multicomponent catalysts calcined at 823 K

Catalyst (molar ratio)	S_{BET} ($m^2\,g^{-1}$)	EB conv. (%)	Selectivity (%)		
			STY	B	T
Mg/Al (2/1)	125.4	6.7	95.6	4.4	0
Mg/Al/Fe (6/2/1)	110.5	30.6	98.9	0.8	0.3
Mg/Al/Fe (6/1.5/1.5)	118.0	34.2	99.3	0.3	0.4
Mg/Al/Fe (6/1/2)	110.8	38.5	99.1	0.6	0.3
Mg/Al/Fe (6/0.5/2.5)	105.0	37.5	98.4	1.0	0.6
Mg/Cu/Al/Fe (3/3/1/2)	85.5	30.6	98.3	1.0	0.7
Mg/Mn/Al/Fe (3/3/1/2)	105.5	34.1	98.2	1.2	0.6
Mg/Ni/Al/Fe (3/3/1/2)	147.3	49.3	80.5	17.7	1.8
Mg/Co/Al/Fe (3/3/1/2)	98.4	47.3	98.7	0.8	0.5
Mg/Zn/Al/Fe (3/3/1/2)	90.8	53.8	96.7	2.7	0.6

Reaction conditions: 200 mg catalyst; N_2:CO_2:EB = 36:19:1; 773 K; 2 h on stream. EB, ethylbenzene; STY, styrene; B, benzene; T, toluene.

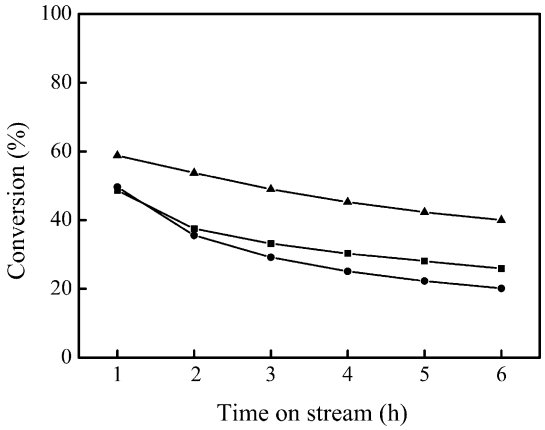

Fig. 4. Effect of reaction time on EB conversion at 773 K. (●) Mg/Fe (2/1) catalyst; (■) Mg/Al/Fe (6/0.5/2.5) catalyst; (▲) Mg/Zn/Al/Fe (3/3/1/2) catalyst.

performance is described in Table 2. The catalytic activity of the catalysts decreases in the order of Mg/Zn/Al/Fe > Mg/Ni/Al/Fe > Mg/Co/Al/Fe > Mg/Al/Fe > Mg/Mn/Al/Fe > Mg/Cu/Al/Fe. Obviously, some of them are more active than the Mg/Fe catalyst, in particular the Mg/Zn/Al/Fe catalyst displaying a maximum EB conversion of 53.8% and a styrene selectivity of 96.7%. Under similar reaction conditions, the Mg/Zn/Al/Fe catalyst seems even more active for EB dehydrogenation in the presence of CO_2 than the Mg/V/Al catalyst reported in a recent literature [15].

The effect of reaction time on EB conversion over some representative catalysts is shown in Fig. 4. The Mg/Fe catalyst deactivates rather fast in the first 3 h and then becomes almost stable. Comparing the activity change with time of the three catalysts shows that the incorporation of Zn^{2+} and Al^{3+} into the catalysts not only increases the dehydrogenation activity but also improves the catalyst stability. The Mg/Al/Fe and Mg/Zn/Al/Fe catalysts are almost stable after 2 h on stream. A regeneration treatment of the catalysts after 6 h reaction at 773 K was attempted. As shown in Fig. 5, EB

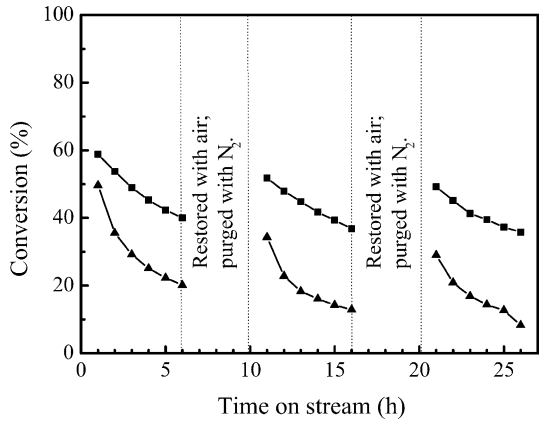

Fig. 5. Regeneration of catalysts used for EB dehydrogenation at 773 K. (■) Mg/Zn/Al/Fe (3/3/2/1); (▲) Mg/Fe (2/1).

Table 3
Effects of reaction temperature and pretreatment atmosphere on catalytic properties of Mg/Zn/Al/Fe (3/3/1/2) catalyst

Temperature (K)	Pretreatment gas	EB conv. (%)	Selectivity (%)		
			STY	B	T
723	N_2	25.6	98.1	1.9	0
773	N_2	53.8	96.7	2.7	0.6
823	N_2	68.2	96.0	2.7	1.3
773	H_2	46.1	96.8	2.6	0.6

Reaction conditions: 200 mg catalyst; N_2:CO_2:EB = 361:19:1; 773 K; 2 h on stream. EB, ethylbenzene; STY, styrene; B, benzene; T, toluene.

conversions on Mg/Zn/Al/Fe and Mg/Fe catalysts decrease from 58.8 and 49.6% at 1 h to 40.0 and 20.1% at 6 h, respectively. The reaction was interrupted under a nitrogen stream, and then air was introduced to burn off carbon species deposited on the catalysts. After air treatment at 773 K for 2 h, the catalysts were purged with N_2 for 2 h. The EB conversions on the regenerated catalysts are lower than the initial conversions, showing that the original activity of the catalysts could not be fully restored. Meanwhile, after the second regeneration the activity of Mg/Zn/Al/Fe catalyst is almost fully restored, while the Mg/Fe catalyst exhibits a conversion slightly lower than that after the first regeneration. The increase in activity after regeneration is due to the removal of the carbonaceous deposit on the catalysts. The difference in the regeneration behavior between the two catalysts indicates that the Mg/Zn/Al/Fe catalyst has a higher catalytic stability than the Mg/Fe catalyst.

Table 3 summarizes the effects of reaction temperature and pretreatment atmosphere on the catalytic properties of Mg/Zn/Al/Fe catalyst. The dehydrogenation activity increases significantly with the increase of reaction temperature, but the selectivity to styrene is slightly decreased. The amount of benzene and toluene in the reaction product is increased, showing that cracking reaction is favored at higher temperature. The catalyst pretreatment atmosphere has an evident effect on the activity of the catalyst. Prereduction of the catalyst is undesirable for the reaction.

In order to understand the role of CO_2 in the reaction, the variation of the amount of CO in the reaction product with reaction time on Mg/Zn/Al/Fe catalyst was tested and given in Fig. 6. The amount of CO formed in the reaction is only slightly lower than that of styrene at the beginning, but it decreases gradually with reaction time. This suggests that both oxidative dehydrogenation and simple dehydrogenation reaction are probably present on the catalyst, as shown below:

$$C_6H_5–C_2H_5 + CO_2 \rightarrow C_6H_5–CH{=}CH_2 + CO + H_2O$$

$$C_6H_5–C_2H_5 \rightarrow C_6H_5–CH{=}CH_2 + H_2$$

Although oxidative dehydrogenation dominates at the initial stage of the reaction, it is accompanied by simple dehydrogenation as time goes on. The carbonaceous deposit

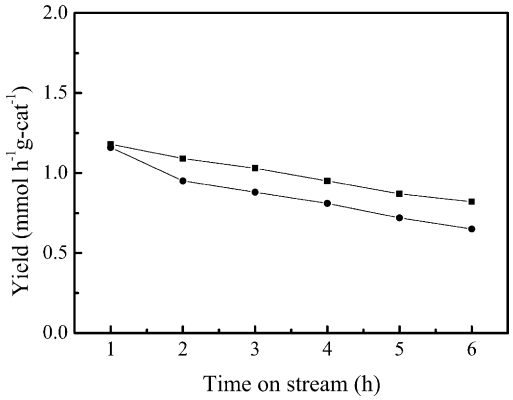

Fig. 6. Yield of styrene and CO in the reaction course on Mg/Zn/Al/Fe (3/3/1/2) catalyst at 773 K. (■) Styrene; (●) CO.

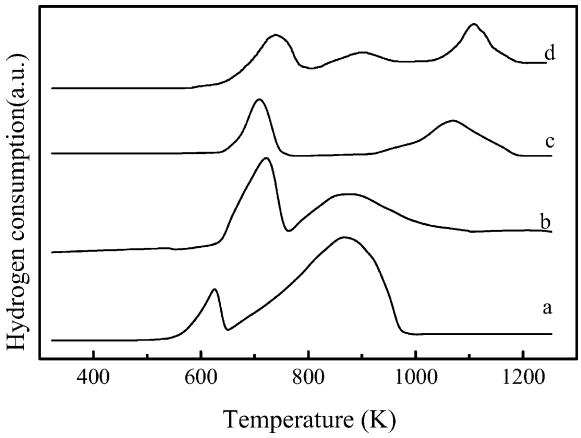

Fig. 7. TPR profiles of the catalysts. (a) α-Fe_2O_3; (b) Mg/Fe (2/1); (c) Mg/Al/Fe (6/1/2); (d) Mg/Zn/Al/Fe (3/3/1/2).

on the catalyst surface or the poisoning of some oxidative dehydrogenation sites by CO might be the reason for the change of reaction mechanism. This deserves further studies.

3.3. Acid–base properties

NH_3-TPD and CO_2-TPD methods were used to measure the acid–base properties of some representative catalysts and the results were listed in Table 4. Incorporation of Zn^{2+} and Al^{3+} into the catalyst increases the amount of stronger acid sites and the total amount of base sites on the catalyst surface. Mg/Zn/Al/Fe catalyst is abundant in stronger acid sites and has a moderate amount of base sites in comparison with the other two catalysts.

The oxidative dehydrogenation of EB is suggested by various authors [16–19] to proceed through the following steps: the adsorption of EB on an acid site, the abstraction of α-hydrogen from EB by a basic OH group adjacent to the acid site, the formation of an anion vacancy via desorption of water, the filling of the vacancy site by O^- species formed from adsorbed O_2 or CO_2 and the abstraction of β-hydrogen from EB by the O^- species to give styrene and basic OH group. According to this reaction mechanism, both acid and base sites are necessary for the reaction. The large number of stronger acid sites on Mg/Zn/Al/Fe catalyst enhances the adsorption and activation of EB molecules, and the availability of adjacent basic OH groups on the catalyst promotes the abstraction of α-hydrogen from EB molecules to form water. This may constitute one of the reasons for the enhanced dehydrogenation activity of the Mg/Zn/Al/Fe catalyst.

3.4. TPR study

The TPR profiles of α-Fe_2O_3 and the representative catalysts are illustrated in Fig. 7. There are two reduction peaks on the profile of α-Fe_2O_3, corresponding to the reduction of α-Fe_2O_3 to Fe_3O_4 and Fe, respectively [20]. The TPR profile of Mg/Fe catalyst looks similar to that of α-Fe_2O_3, except that the first peak temperature is increased. However, the reduction of Mg/Al/Fe and Mg/Zn/Al/Fe catalysts gives a different picture. The second reduction peaks on the profiles of these catalysts shift to temperatures well above 1000 K.

It has been suggested that the iron oxide species, such as ferrites, composite oxide or magnetite, are the active components in this type of catalysts for oxidative dehydrogenation of EB in the presence of CO_2 [1,2,4,5,21]. The iron oxide species take part in the redox cycle with EB and CO_2 in the reaction. Our experimental results seem to support this postulation, since the dehydrogenation activity increases with the amount of iron oxide in the catalysts and prereduction with H_2 deteriorates the catalytic activity of the catalysts. Based on this postulation as well as the TPR results, the increase in catalytic activity and stability of the catalysts after incorporation of Zn^{2+} and Al^{3+} can also be ascribed to the restricted reduction of the iron oxide species under reaction conditions besides their favorable acid–base properties.

Table 4
Acid–base properties of some representative catalysts

Catalyst (mmol g^{-1})	Peak temperature (K)		NH_3 desorbed		Peak temperature (K)		CO_2 desorbed (mmol g^{-1})	
	I	II	I	II	I	II	I	II
Mg/Fe (2/1)	538	–	0.310	–	441	543	0.003	0.036
Mg/Al/Fe (6/1/2)	513	668	0.394	0.214	444	547	0.010	0.100
Mg/Zn/Al/Fe (3/3/1/2)	463	588	0.150	0.310	453	653	0.034	0.019

4. Conclusions

A series of Fe-containing HTlcs were prepared by coprecipitation method. Mg/Fe catalysts prepared by calcination of the hydrotalcite-like precursors have high specific surface areas and are active catalysts for the dehydrogenation of EB in the presence of CO_2. Incorporation of Al^{3+}, Ni^{2+}, Co^{2+}, and Zn^{2+} into the HTlcs increases the dehydrogenation activity of the catalysts. The Mg/Zn/Al/Fe (3/3/1/2) catalyst exhibits the highest EB conversion of 53.8% at 773 K with a styrene selectivity of 96.7%. Slower deactivation is observed on Mg/Zn/Al/Fe catalyst than Mg/Fe catalyst, and the activity of the catalyst can be restored after burning of the carbonaceous deposit.

The amount of CO produced during the reaction agrees well with the amount of styrene at the initial stage of the reaction on Mg/Zn/Al/Fe catalyst, but is reduced by a factor of 44% as reaction goes on, indicating that the oxidative dehydrogenation reaction is probably accompanied with the simple dehydrogenation reaction to a minor extent.

Acid–base measurements of the catalysts reveal that the existence of a larger amount of stronger acid sites and a moderate amount of base sites accounts for the high dehydrogenation activity of Mg/Zn/Al/Fe catalyst. TPR studies show that the reduction of the iron oxide species in the catalysts is retarded after the incorporation of Zn^{2+} and Al^{3+}. The restricted reduction of iron oxide species under the reaction conditions favors the redox cycle in the reaction and enhances the catalytic activity and stability of Mg/Zn/Al/Fe catalyst.

Acknowledgements

The work was supported by the Chinese Major State Basic Research Development Program (Grant 2000077507), Shanghai Research Institute of Petrochemical Technology and the Shanghai Major Basic Research Program (03DJ14004).

References

[1] N. Mimura, I. Takahara, M. Saito, T. Hattori, K. Ohkuma, M. Ando, Catal. Today 45 (1998) 61.
[2] M. Sugino, H. Shimada, T. Turuda, H. Miura, N. Ikenaga, T. Suzuki, Appl. Catal. A 121 (1995) 125.
[3] T. Badstube, H. Papp, P. Kustrowski, R. Dziembaj, Catal. Lett. 55 (1998) 169.
[4] N. Mimura, M. Saito, Catal. Lett. 58 (1999) 59.
[5] T. Badstube, H. Papp, R. Dziembaj, P. Kustrowski, Appl. Catal. A 204 (2000) 153.
[6] Y. Sakurai, T. Suzaki, N. Ikenaga, T. Suzuki, Appl. Catal. A 192 (2000) 281.
[7] Y. Sakurai, T. Suzaki, K. Nakagawa, N. Ikenaga, H. Aota, T. Suzuki, Chem. Lett. (2000) 526.
[8] Y. Sakurai, T. Suzaki, K. Nakagawa, N. Ikenaga, H. Aota, T. Suzuki, J. Catal. 209 (2002) 16.
[9] V.P. Vislovskiy, J.-S. Chang, M.-S. Park, S.-E. Park, Catal. Commun. 3 (2002) 227.
[10] J.-N. Park, J. Noh, J.-S. Chang, S.-E. Park, Catal. Lett. 65 (2000) 75.
[11] J. Noh, J.-S. Chang, J.-N. Park, K.Y. Lee, S.-E. Park, Appl. Organometal. Chem. 14 (2000) 815.
[12] N. Ikenaga, T. Tsuruda, K. Senma, T. Yamaguchi, Y. Sakurai, T. Suzuki, Ind. Eng. Chem. Res. 39 (2000) 1228.
[13] F. Cavani, F. Trifiro, A. Vaccori, Catal. Today 11 (1991) 173.
[14] N. Mimura, I. Takahara, M. Saito, Y. Sazaki, K. Murata, Catal. Lett. 78 (2002) 125.
[15] G. Carja, R. Nakamura, T. Aika, H. Niiyama, J. Catal. 218 (2003) 104.
[16] T. Tagawa, T. Hattori, Y. Murakami, J. Catal. 75 (1982) 66.
[17] T.M. Jyothi, K. Sreekumar, M.B. Talawar, A.A. Belhekar, B.S. Rao, S. Sugunan, Bull. Chem. Soc. Jpn. 73 (2000) 1285.
[18] S. Sugunan, N.K. Renuka, Bull. Chem. Soc. Jpn. 75 (2002) 463.
[19] V.M. Zhyznevskiy, R.D. Tsybokh, V.V. Gumenetsikiv, V.V. Kochubeiy, Appl. Catal. A 238 (2003) 19.
[20] Z. Gao, B. Zhang, J. Cui, Appl. Catal. 72 (1991) 331.
[21] H. Shimada, T. Akazawa, N. Ikenaga, T. Suzuki, Appl. Catal. A 168 (1998) 243.